Food Hydrocolloids 135 (2023) 108119

Contents lists available at ScienceDirect

Food Hydrocolloids

journal homepage: www.elsevier.com/locate/foodhyd

Tailoring structural, rheological and gelling properties of watermelon rind pectin by enzymatic treatments

D.A. Méndez [a,b], A. Martínez-Abad [a,c], M. Martínez-Sanz [c,d], A. López-Rubio [a,c], M.J. Fabra [a,c,*]

[a] Food Safety and Preservation Department, Institute of Agrochemistry and Food Technology (IATA-CSIC), Valencia, Spain
[b] Grupo de investigación Bioecono, Facultad de ciencias económicas y administrativas, Universidad del Tolima, Tolima, Colombia
[c] Interdisciplinary Platform for Sustainable Plastics towards a Circular Economy- Spanish National Research Council (SusPlast-CSIC), Madrid, Spain
[d] Instituto de Investigación en Ciencias de la Alimentación, CIAL (CSIC-UAM, CEI UAM + CSIC), Nicolás Cabrera, 9, 28049, Madrid, Spain

ARTICLE INFO

Keywords:
Scattering
Enzymes
SAXS
Rheology
Gelation

ABSTRACT

In this work, pectin extracts from watermelon rind (WRP) were enzymatically treated to evaluate their potential for preparing hydrogels with the addition of $CaCl_2$. Based on a previous work, two different conditions were selected to obtain WRP extracts according to the 1) highest yield (OP) or 2) highest yield without negatively affecting the branching and native structure of pectin (OPA). Firstly, both WRP extracts were enzymatically modified using different treatments (de-esterification and/or de-branching of galacturonic and arabinose side chains, and deproteinization), and their impact on the esterification degree, monosaccharide composition and changes on their structural properties (linearity and branching degree) were analysed. Then, the effect of the structural properties of the resulting pectin on the rheological behaviour and nanostructure of the hydrogels was investigated. The presence of long branched side chains and high methyl-esterified galacturonic acid chains promoted the formation of weaker hydrogels whereas de-esterification of the original pectin enabled intermolecular association giving rise to stronger hydrogels with the formation of ordered and densely packed structures (as deduced from SAXS results). However, the presence of small arabinogalactans side chains in the de-branched and de-esterified pectin extracts acted as reinforcement agents, inducing the formation of more densely packed networks and stronger hydrogels than their less-branched counterpart. These results demonstrated the impact of the pectin structure on the hydrogel-forming capacity.

Author statement

D.A. Méndez: Methodology, Investigation, Formal analysis, Writing - original draft. A Martinez-Abad: Conceptualization, Methodology, Writing - review & editing. M. Martínez-Sanz: Methodology, Supervision, formal analysis, writing-review & editing. A. López-Rubio: Conceptualization, Methodology, Funding acquisition, Project administration, Writing- Review & Editing. M.J. Fabra: Conceptualization, Methodology, Supervision, Writing - review & editing.

1. Introduction

Pectin is a family of complex heteropolysaccharides consisting of homogalacturonan (HG), rhamnogalacturonan I (RG-I) and rhamnogalacturonan II (RG-II). HG is a linear chain of 1,4 – linked α-D- galacturonic acid (GalA) residues, which can be methoxylated at C-6 and/or acetylated on the O-2 and/or O-3 position. The degree and distribution of methoxylation are important parameters for their gelling properties (Ngouémazong et al., 2012; Voragen, Coenen, Verhoef, & Schols, 2009). HG is often referred to as the pectin smooth region, whereas RG-I is called the hairy region since its backbone can be abundantly substituted by neutral sugars like arabinose and galactose forming arabinan, galactan and arabinogalactans on the side chains, predominantly attached to the O-4 position of rhamnose (Lara-Espinoza, Carvajal-Millán, Balandrán-Quintana, López-Franco, & Rascón-Chu, 2018). In contrast, RG-II is composed of a HG backbone, which is branched with chains at C-2 and C-3. These side chains include arabinose, fucose, galactose, rhamnose, glucuronic acid, galacturonic acid, xylose, apiose and fucose units.

The worldwide application of pectin in the food industry as gelling, thickening, and stabiliser agents (Schols & Voragen, 2003a) together with the global aim towards sustainability, has prompted the interest in

* Corresponding author. Food Safety and Preservation Department, Institute of Agrochemistry and Food Technology (IATA-CSIC), Valencia, Spain.
E-mail address: mjfabra@iata.csic.es (M.J. Fabra).

https://doi.org/10.1016/j.foodhyd.2022.108119
Received 2 May 2022; Received in revised form 16 August 2022; Accepted 2 September 2022
Available online 13 September 2022

valorising by-products or residues from the food chain to find new pectin sources following circular economy principles. Specifically, watermelon (*Citrillus lanatus*), has been considered a promising pectin source, ascribed to the high amounts of biomass waste generated by the global production that accounts 100 million tonnes in 2019 (FAOSTAT, 2021), of which one third (rind) is discarded (Petkowicz, Vriesmann, & Williams, 2017). Although different approaches for the extraction and characterization of watermelon rind pectin (WRP) have been proposed and discussed in the literature (Campbell, 2006; Hartati & Subekti, 2015; Lee & Choo, 2020; Méndez, Fabra, Gómez-Mascaraque, López-Rubio, & Martinez-Abad, 2021; Petkowicz et al., 2017; Prakash Maran, Sivakumar, Thirugnanasambandham, & Sridhar, 2014), the understanding of the relationship between watermelon pectin structure and functionality could provide an opportunity to customize their functional and technological properties depending on the final application.

In a previous work, a Box–Behnken response surface experimental design was carried out to optimize the pectin extraction process from watermelon rind (Méndez, Fabra, Gómez-Mascaraque et al., 2021) and, the conditions in which the yield was the highest (OP) were used to evaluate the emulsifying properties of this pectin extract. The compositional features showed relevant structural differences compared to other conventional pectin, related to the higher content of neutral sugars. At optimum yield conditions, WRP yield (13.4%), purity (464.6 μg/g galacturonic acid) and molar mass (106.1 kDa) were comparable to traditional pectin sources but showed branching degree with longer galactan side chains and higher protein interaction (Méndez, Fabra, Gómez-Mascaraque et al., 2021; Méndez, Fabra, Martínez-Abad et al., 2021). Its greater emulsifying capacity as compared to commercial citrus or apple pectin was ascribed to the presence of longer side chains in the WRP combined with its relatively high protein content (mainly acting as the surface-active material) (Méndez, Fabra, Martínez-Abad et al., 2021).

Pectin-modifying enzymes are of great interest to make controlled changes on the molecular structure of this polysaccharide and several works have reported about the effects of side chain- and backbone-modifying enzymes on i) the composition and structure of pectin, ii) the rheological behaviour of the resulting pectin dispersions and iii) the gelling capacity of the corresponding gels (Funami et al., 2007, 2011; Nakauma et al., 2008). In this study, the gelling capacity of WRP before and after enzymatic treatments was explored. In contrast to previous studies, the aim of the present work was not only to investigate the effect of controlled enzymatic debranching, de-esterification and protein removal on watermelon rind pectin composition and molecular structure but also to deeply characterize the structure of the pectin hydrogels using small angle X-ray scattering (SAXS) and rheology, in order to understand the role of the RG-I side chains and protein moieties on the molecular structure of the gel of the resulting pectin.

2. Materials and methods

2.1. Sample preparation

Fresh watermelon (*Citrullus lanatus*) fruits were kindly supplied by Anecoop S. Coop. during the summer season of 2019 from Almeria, Spain. The fruits were processed removing the red flesh and keeping the rind, which were later used for pectin extraction. The rinds were initially chopped in pieces of 0.5–2.5 cm and immersed in distilled water for 10 min with gentle agitation and, after draining the water, they were freeze-dried to keep them stable before pectin extraction. Sodium hydroxide (pharma grade) and hydrochloric acid was supplied by Sigma-Aldrich (Stenheim, Germany). Acetone (99%) and ethanol (96% v/v, USP grade) were purchased from WVR chemicals and Panreac Applichem (Darmstadt, Germany), respectively. The enzymes pectin methylesterase (PME) from orange peel (≥150 units/mg protein), alcohol oxidase solution from *Pichia pastoris* (EC 1.1.3.13), pepsin (EC 3.4.23.1), protease from *Aspergillus oryzae* (EC 232.752.2), 2,4-pentanedione (≥99%) and the analytical standards: D-(+)-galactose, D-(+)-galacturonic acid monohydrate, L-rhamnose monohydrate, D-glucuronic Acid D-(+)-mannose, D-(+)-glucose, D-(−)-fructose, L-(−)-fucose, D-(+)-xylose, L-(+)-arabinose were all purchased from Sigma-Aldrich (St. Louis, Missouri, USA). Polygalacturonic acid from citrus pectin low methoxy (5%) (LMCP), endo-1,5-α-arabinanase (EAR) (*Aspergillus niger*, EC 3.2.1.99) and endo-1,4-β-galactanase (EGA) (*Aspergillus niger*, EC 3.2.1.89), were supplied by Megazyme Ltd. (Wicklow, Ireland).

2.2. Pectin extraction

Following the Box–Behnken response surface experimental design carried out to optimize the pectin extraction process from watermelon rind (Méndez, Fabra, Gómez-Mascaraque et al., 2021), two different conditions were selected for this work: i) where the yield was the highest (OP) (95 °C pH 1.36 and 90 min) and, ii) where the yield was the highest without negatively affecting the branching and native structure of pectin (OPA) (81.7 °C pH 2.15 and 90 min). Briefly, the ground watermelon rind was immersed in water and acidified using a 1 M HCl solution, with a solid-liquid ratio of 1:20 (w/v). Subsequently, after acid extraction the extracted solution was filtered with a muslin cloth, followed by vacuum filtration using Whatman filter paper nº 4 at 60 °C, mixed with 96% (v/v) ethanol at a 1:3 (v/v) ratio and left overnight in the freezer. The coagulated pectin (WRP) was centrifuged at 12000 rpm for 20 min and consecutively washed with 96% (v/v) ethanol and acetone twice to remove water and low molecular weight or polar compounds. Finally, the material was dried at 60 °C in a hot air oven until constant weight, then grounded and stored in a desiccator until further analysis.

2.3. Preparation of enzymatically modified pectin samples

Both pectin extracts (OP and OPA) were enzymatically modified using six different treatments. Briefly, stock solutions of each pectin extract were prepared by dispersing 1% (w/v) in 100 mM PBS (pH 7.2) or in 100 mM citrate buffer (pH 4.0), overnight, under gentle magnetic stirring. These two stock solutions were prepared according to the optimum pH conditions provided by the supplier: PME optimum pH was around the neutral whereas EGA, EAR, pepsin and proteases were active at pH 4.0. The enzymes were added and incubated at 40 °C for 24 h under gentle stirring, as described below and with the following aims:

i) De-esterification: PME (10 units per 1.0 g WRP) was incorporated in the pectin solutions prepared with PBS. Potential side activities of PME due to lack of purity were ruled out as no increase in reducing sugars was noted, following the 3,5- dinitrosalicilic colorimetric assay.
ii) De-branching of galacturonic side chains: EGA (10 units per 1.0 g WRP) was added to the pectin solutions prepared with citrate buffer.
iii) De-branching of arabinose side chains: EAR (10 units per 1.0 g WRP) was dissolved in the pectin/citrate buffer-stock solutions.
iv) De-esterification and de-branching of galacturonic side chains: EGA and PME were used at the concentrations reported for i) and ii) and gently stirred in the pectin/PBS-stock solutions.
v) De-esterification and de-branching of arabinose side chains: EAR and PME were dissolved in pectin/PBS-stock solutions and used at the concentrations stated at i) and iii).
vi) Deproteinization: pectin/citrate buffer stock solutions were used and, both pepsin (700 unit per 1.0 g WRP) and protease (70 unit per 1.0 g WRP) (PP) were added and incubated at 40 °C for 24 h with gentle stirring.

All enzyme-treated pectin solutions were heated at 90 °C for 5 min to stop the enzymatic reaction. The resulting solutions were then rapidly cooled in an ice bath and dialyzed against deionized water at 20 °C

through a dialysis membrane with a 3.5 kDa molecular weight cut-off, followed by freeze-drying. The freeze-dried samples were stored in a desiccator at 20 °C until analysis. Sample's nomenclature was "*x*-*y*' where '*x*' refers to the type of pectin extract, and "*y*" specifies the enzymes used for each treatment.

2.4. Compositional characterization

2.4.1. Monosaccharide composition

The sugar composition of the samples was determined after acidic methanolysis as previously described by Méndez, Fabra, Gómez-Mascaraque, et al. (2021). The monosaccharides were analysed using high performance anion exchange chromatography with pulsed amperometric detection (HPAEC-PAD) with an ICS-6000 system (Dionex) equipped with a CarboPac PA1 column (4 × 250 mm, Dionex). Control samples of known concentrations of mixtures of glucose (Glc), fucose (Fuc), rhamnose (Rha), galactose (Gal), arabinose (Ara), xylose (Xyl), mannose (Man), galacturonic acid (GalA) and glucuronic acid (GlcA) were used for calibration.

2.4.2. Determination of the degree of esterification (DE)

The DE of all pectin samples was calculated as the ratio of the molar number of methyl-groups (as methanol) to the molar amount of GalA estimated per gram of sample and expressed in percentage. The methyl esters of all pectin samples were hydrolysed and the methanol produced during pectin saponification was determined based on a colorimetric method (Klavons & Bennett, 1986). The GalA content of the pectin was taken from monosaccharide composition. All concentrations were determined on dry basis.

2.4.3. Protein content

The protein content of the two pectin types was analysed for total nitrogen content using an Elemental Analyser Rapid N Exceed (Paralab S.L., Spain). About 100 mg of each of the powdered samples were pressed to form a pellet which was then analysed using the Dumas method, which is based on the combustion of the sample and subsequent detection of the released N_2 (Wiles et al., 1998). The total protein content was calculated from the nitrogen content multiplied by a factor of 6.25.

2.5. Rheological characterization

2.5.1. Flow-curves of pectin solutions

The viscosity of the pectin solutions was analysed using a rheometer HR20, (TA Instruments, Montreal, QC, Canada) with a 40 mm parallel plate geometry. Briefly, pectin solutions at 2% (w/v) were dissolved in Milli-Q water (18.2 MΩ cm resistance, Millipore, USA). Samples were loaded on the bottom of a Peltier plate. The viscosity was measured by applying a rotational shear between the two parallel plates at 20 °C with a gap of 500 μm as a function of increasing shear rate from 0.1 s^{-1} to 200 s^{-1}. The rheological behaviour of the samples was recorded with the TRIOS software version 5.1.1.46572 (TA Instruments, Montreal, QC, Canada). The power law model Eq. (1) was applied to determine the consistency index (k) and the flow behaviour index (n). The apparent viscosities were determined at 100 s^{-1}.

$$\sigma = K\,\gamma^{n} \quad \text{(Eq. 1)}$$

2.5.2. Preparation of Ca^{2+} pectin hydrogels

Each pectin sample was initially dissolved in Milli-Q water (18.2 MUcm resistance, Millipore, USA) in order to obtain 1% (w/v) pectin solutions. The pH of the solution was adjusted to 5.0 using NaOH solutions of concentrations varying from 0.1 to 1 M, and under continuous vigorous stirring. The resulting solutions were immediately used for gel preparation.

Then, a 3 M $CaCl_2$ stock solution was prepared using Milli-Q water. Prior to its use, this stock solution was diluted so as to produce gels with defined Ca^{2+} concentration expressed as the stoichiometric ratio ($R = 2[Ca^{2+}]/[COO^{-}]$) (Capel, Nicolai, Durand, Boulenguer, & Langendorff, 2006). The R-value of each prepared gel was 2.0.

Ca^{2+} pectin gels were prepared on the lower plate of a stress controlled HR20, rheometer (TA Instruments, Montreal, QC, Canada). A few microliters of pectin and $CaCl_2$ solutions were preheated to 50 °C. Meanwhile, the Peltier controlled lower plate of the rheometer was preheated to 50 °C. Specifically, 670 μL of the pre-heated pectin solution were placed at the centre of the lower plate. Subsequently, 35 μL of the preheated $CaCl_2$ was added dropwise over the entire pectin surface. The upper geometry (40 mm parallel plate) was then lowered to the set measuring gap (0.5 mm). The edge of the sample was covered with a layer of paraffin oil to prevent evaporation during gel formation and measurements. To limit temperature fluctuations within the sample, the upper plate was preheated and lowered over the loaded sample.

2.5.3. Small-amplitude oscillatory shear tests

The loaded (time zero of the experiment) sample with Ca^{2+} cations mixed was allowed to equilibrate for 5 min (to ensure complete calcium diffusion through the 670 μL pectin solution), and was subsequently cooled to 20 °C at a rate of 6 °C/min. After that, the sample was maintained for 1 h at 20 °C to ensure a complete gel formation. Before measurements, linear viscoelastic sweeps were performed from 0.01 to 100% strain at a frequency of 1 rad/s, in order to define the linear viscoelastic region of the gels at 20 °C. A dynamic viscoelastic test was conducted in the frequency range from 0.01 to 100 rad/s, and the viscoelastic properties (storage moduli -G'- and loss moduli -G''-) of the hydrogels were recorded as a function of the frequency. Although the aforementioned gel preparation method and rheological measurements have been reported to be reproducible (Doungla & Vandebril, 2009), all experiments were performed in duplicate, on freshly prepared gels.

2.6. Fourier transform infrared (FTIR)

The IR spectra of samples were measured in the wavenumber range of 600–4000 cm^{-1} by a Jasco FT-IR-4100 spectrometer (Tokyo, Japan) coupled with a TGS detector. The spectral resolution was 4 cm^{-1}. Each spectrum was the average of 32 scans. During the whole experiment, the temperature was kept at about 25 °C and the humidity was kept at a stable level in the laboratory.

2.7. SAXS analysis of pectin hydrogels

SAXS experiments were carried out in the Non-Crystalline Diffraction beamline, BL-11, at ALBA synchrotron light source (www.albasynchrotron.es). Briefly, the samples were prepared at 1% (w/v), following the same procedure in section 2.5.2. Initially, the $CaCl_2$ solution was added to the capillaries keeping the same stoichiometric ratio as commented before for the rheology measurements. Then, the pectin solution was slowly added to obtain the hydrogel inside the capillary. The samples were placed in sealed 2 mm quartz capillaries (Hilgenberg GmbH, Germany). The energy of the incident photons was 12.4 KeV or equivalently a wavelength, λ, of 1 Å. The SAXS diffraction patterns were collected by means of a photon counting detector, Pilatus 1M, with an active area of 168.7 × 179.4 mm^2, an effective pixel size of 172 × 172 μm^2 and a dynamic range of 20 bits. The sample-to-detector distance was set to 7570 mm, resulting in a q range with a maximum value of $q = 0.19$ $Å^{-1}$. An exposure time of 10 s was selected based on preliminary trials. The data reduction was treated by pyFAI python code (ESRF) (Kieffer & Ashiotis, 2014), modified by ALBA beamline staff, to do on-line azimuthal integrations from a previously calibrated file. The calibration files were created from a silver behenate (AgBh) standard. The intensity profiles were then represented as a function of q using the

IRENA macro suite (Ilavsky & Jemian, 2009) within the Igor software package (Wavemetrics, Lake Oswego, Oregon).

The scattering patterns were properly described using different fitting functions depending on the sample: (i) correlation length, (ii) two-level unified model or (iii) three-level unified model.

The correlation length model is described by the following equation:

$$I(q) = \frac{A}{q^n} + \frac{C}{1 + (q\xi_L)^m} + bkg \quad \text{(Eq. 2)}$$

The first term in equation (2) is described by a power-law function and accounts for the scattering from large clusters in the low q region, while the second term, consisting of a Lorentzian function, describes scattering from polymer chains in the high q region. n is the power-law exponent, A is the power-law coefficient, m is the Lorentzian exponent, C is the Lorentzian coefficient and ξ_L is the correlation length for the polymer chains (which gives an indication of the gel's mesh size). The third term accounts for the incoherent background.

The unified model considers that, for each individual level, the scattering intensity is the sum of a Guinier term and a power-law function (Beaucage, 1995, 1996):

$$I(q) = \sum_{i=1}^{N} G_i \exp\left(-q^2 \cdot \frac{R_{g,i}^2}{3}\right) + \frac{B_i\left[erf\left(qR_{g,i}/\sqrt{6}\right)\right]^{3P_i}}{q^{P_i}} + bkg \quad \text{(Eq. 3)}$$

where $G_i = c_i V_i \Delta SLD_i^2$ is the exponential prefactor (where V_i is the volume of the particle and ΔSLD_i is the scattering length density (SLD) contrast existing between the ith structural feature and the surrounding solvent), $R_{g.i}$ is the radius of gyration describing the average size of the ith level structural feature, B_i is a q-independent prefactor specific to the type of power-law scattering with power-law exponent, P_i, and *bkg* is the background. In this particular case, the two (i = 2) or three (i = 3) levels were considered, depending on the sample. In all cases, the largest structural level was modelled only by a power-law (R_{g1} was fixed at a value $\gg q_{min}^{-1}$ of 5000 Å).

The obtained values from the fitting coefficients are those that minimize the value of Chi-squared, which is defined as:

$$\chi^2 = \sum \left(\frac{y - y_i}{\sigma_i}\right)^2 \quad \text{(Eq. 4)}$$

where y is a fitted value for a given point, y_i is the measured data value for the point and σ_i is an estimate of the standard deviation for y_i. The curve fitting operation is carried out iteratively and for each iteration, the fitting coefficients are refined to minimize χ^2.

2.8. Statistical analysis

All statistical analysis was performed using the statistical software Statgraphics Centurion XVI® (Manugistics Inc.; Rockville, MD, USA). Statistically significant differences were determined by using one-way analyses of variance (ANOVA) and sample comparison with LSD at 95% confidence level (*p-value* < 0.05).

3. Results and discussion

3.1. Sugar constituents, composition and structure of the enzymatically-treated WRP extracts

Compositional and structural analyses were firstly carried out on WRP extracts (OP and OPA) and on the resulting enzymatically-treated pectin samples. Sugar ratios were also calculated based on previous literature (Denman & Morris, 2015; Houben, Jolie, Fraeye, Van Loey, & Hendrickx, 2011; Méndez, Fabra, Gómez-Mascaraque et al., 2021; Ognyanov et al., 2018) to estimate the linearity (RL) and branching (RB) degree of the various pectin and, thus, to get a better understanding on their structural differences. Table 1 summarizes the results from the compositional analysis. When comparing OPA and OP, it was clearly seen that the branching degree and relative content of Ara was significantly higher in OPA, and suggests the presence of high and long distribution of arabinan and/or arabinogalactan side chains. This is explained by the harsher acid conditions in the extraction process, which are known to more specifically cleave the neutral sugar side chains, especially arabinosyl residues (Méndez, Fabra, Gómez-Mascaraque et al., 2021; Ngouémazong et al., 2012; Schols & Voragen, 2003b; Verhoef, Lu, Knox, Voragen, & Schols, 2009). As reported in our previous works, WRP generally displayed a lower rhamnose content compared to typical industrial pectin from citrus or apple. In this sense, the relative content of Rha was even lower in OPA than in OP, suggesting the presence of longer sugar side chains in the rhamnogalacturonan (RG-I) region. Furthermore, the protein content was significantly higher in OPA, ascribed to the milder extraction conditions used in this case and attributed to the protein interaction with

Table 1
Chemical composition and sugar content of the different enzymatic treatments (pectin methyl esterase (PME), endo-1,5-α-arabinanase (EAR), endo-1,4-β-galactanase (EGA), pepsin, protease (PP)) with OP and OPA.

Sample	Protein (%)	DE (%)	Fuc (μg/mg)	Rha (μg/mg)	Ara (μg/mg)	Gal (μg/mg)	GalA (μg/mg)	RB [a]	RL[b]	RG-I %[c]
OPA	18.0(1.5)^{bc}	57.1(4.6)^{c}	5.1(0.4)^{c}	9.4(0.8)^{f}	30.9 (2.7)^{a}	170.9(14.8)^{ab}	345.7(28.9)^{g}	21.38	1.63	20.20
OPA-PME	21.1(2.6)^{a}	3.7(0.1)^{hi}	3.8(1.2)^{hi}	15.2(0.4)^{bc}	25.3(1.8)^{b}	103.5(16.4)^{d}	529.4(0.3)^{a}	8.45	3.67	12.91
OPA-EAR	20.6(3.3)^{ab}	35.9(0.1)^{f}	5.1(0.6)^{f}	11.2(1.0)^{cd}	15.4(0.4)^{d}	163.7(1.8)^{a}	393.9(12.3)^{defg}	16.01	2.07	17.93
OPA-EGA	17.3(0.1)^{c}	33.4(0.4)^{e}	4.9(0.6)^{e}	10.6(0.2)^{ef}	22.9(0.3)^{bc}	149.3(4.2)^{bc}	364.1(1.3)^{fg}	16.27	1.97	17.25
OPA-PME/EAR	19.0(0.2)^{abc}	13.1(0.2)^{i}	1.3(0.1)^{i}	17.5(0.9)^{b}	20(1.0)^{c}	29.1(1.4)^{f}	505.5(24.5)^{ab}	2.80	7.59	4.95
OPA-PME/EGA	19.6(1.7)^{abc}	13.7(0.3)^{h}	1.5(0.1)^{h}	15.6(0.9)^{bc}	24.5(1.3)^{b}	34.1(1.8)^{f}	402.5(20.9)^{defg}	3.76	5.44	5.90
OPA-PP	11.9(1.4)^{d}	42.6(2.6)^{c}	2.5(0.1)^{c}	17.4(1.9)^{b}	29.6(2.8)^{a}	71.0(2.6)^{e}	451.8(53.9)^{abcd}	5.77	3.81	10.09
OP	8.2(0.4)^{e}	50.1(2.1)^{b}	4.8(0.5)^{b}	16.4(4.6)^{a}	0.5(0.9)^{e}	158.8(11.1)^{ab}	464.6(42.2)^{abc}	9.73	2.62	15.97
OP-PME	9.6(0.1)^{de}	4.9(0.1)^{i}	1.0(0.1)^{i}	20.8(0.9)^{a}	1.4(0.1)^{e}	22.9(1.1)^{f}	517.7(23.5)^{a}	1.17	11.52	2.47
OP-EAR	8.2(2.0)^{e}	22.4(0.3)^{d}	2.9(0.2)^{d}	12.1(1.7)^{de}	1.5(0.1)^{e}	90.7(0.2)^{de}	415.8(63.1)^{cdef}	7.59	3.99	9.25
OP-EGA	7.3(0.1)^{e}	31.0(0.6)^{de}	3.9(0.0)^{de}	15.2(1.3)^{bc}	1.3(0.1)^{e}	135.8(2.4)^{c}	367.7(23.2)^{efg}	9.02	2.42	13.74
OP-PME/EAR	9.2(0.4)^{de}	4.8(0.07)^{g}	0.9(0.1)^{g}	11.0(0.6)^{ef}	2.8(0.1)^{e}	28.5(1.5)^{f}	383.5(20.0)^{defg}	2.84	9.08	3.15
OP-PME/EGA	8.1(0.01)^{e}	7.7(0.3)^{g}	0.3(0.4)^{g}	17.2(1.3)^{b}	1.4(0.1)^{e}	14.3(1.6)^{f}	479.6(21.7)^{abc}	0.91	14.44	1.60
OP-PP	8.9(0.8)^{e}	42.6(2.6)^{a}	0.9(0.1)^{a}	20.4(0.1)^{a}	1.3(0.1)^{e}	22.8(0.1)^{f}	393.4(17.01)^{defg}	1.18	8.86	2.45
LMCP[d]	1	5	0	9.07	0.2	9.07	852	1.02	45.45	27.41

Means of each characteristic followed by different letters in the same column (a–j) are significantly different ($p \leq 0.05$), traces or cero values were found for Xyl, Glc, Fru, Man and GlcA.

Values in brackets correspond to standard deviation.

[a] A larger value is indicative of larger average size of the branching side chains. (Gal + Ara/Rha).

[b] A larger value suggests of more linear/less branched pectins. (GalA/(Rha + Ara + Gal)).

[c] (2Rha + Ara + Gal).

[d] LMCP: commercial low methoxy citrus pectin. Data provided by the company.

arabinogalactan side chains in the highly branched structures, as previously reported (Méndez, Fabra, Gómez-Mascaraque et al., 2021).

As seen in Table 1, the treatment with PME had a significant impact on pectin structure, greatly reducing the esterification degree (DE) of the carbohydrates and significantly modifying the composition, linearity and branching ratios. In fact, enzymes with activity on the neutral side chains (EAR and EGA) produced a smaller reduction in Gal and Ara than that of PME. This shows that a pectin structure with long branched chains and a relatively high content of methylated carboxyl groups (>50%) somehow limited the accessibility of the EAR and EGA to the Ara and Gal active sites, as previously stated for carrot, apple and citrus pectin (Funami et al., 2011; Ngouémazong et al., 2012). This effect was more clearly observed for Gal rather than Ara content, probably because Ara units may be more accessible as loose arabinan structures or external arobinosyl residues in the branched side chains. PME catalyses the de-methyl esterification of galacturonic acid units of pectin, generating free carboxyl groups. This may have had an impact on lower molecular weight non-covalently bound neutral sugar chains, resulting in their removal through dialysis. This effect was more patent in the case of the OP extract, probably ascribed to shorter galactan side chains. On the other hand, the combination of PME with enzymes acting on the neutral sugar side chains (PME-EAR and PME-EGA) produced a substantial reduction in both Gal and Ara content. The reduction of Ara in OP samples was not significant due to the negligible quantities in the starting OP sample. This confirms that the PME facilitated the action of EAR and EGA enzymes, more significantly in less branched pectin. Despite the low contents in RG-II (Méndez, Fabra, Gómez-Mascaraque et al., 2021) in WRP, de-branching of pectin with enzymatic treatments was also associated to a decrease in the Fuc content.

Arabinogalactan-proteins (AGP) are widely distributed in plant cell walls, consisting of a protein backbone that is rich in hydroxyproline and to which arabinogalactan polysaccharides are covalently attached, although there are many structural subclasses (Hromadová, Soukup, & Tylová, 2021). This interaction between arabinogalactan and protein moieties has been reported in different studies for sugar beet pectin (Bindereif et al., 2021; Oosterveld, Voragen, & Schols, 2002). The depolymerisation of larger arabinogalactan-protein structures by proteases might result in the removal of smaller protein-carbohydrate fragments through dialysis. As observed in Table 1, the impact of proteolytic enzymes (pepsin and protease; PP) on pectin was clearly demonstrated by a significant decrease in the Gal content for PP-treated pectin. The removal of arabinogalactan- or galactan-protein complexes results in a significant increase in the linearity (RL) in both OP-PP and OPA-PP samples. In OPA-PP samples, a significant reduction in protein content was observed, probably owed to the initial higher protein content. In OP-PP samples, protein content was not significantly reduced, suggesting both protein and carbohydrates (AGP fragments) were removed in equal amounts. This further explains a higher impact in the branching degree of OP-PP compared to OPA-PP samples.

FT-IR analyses were also carried out to assess the compositional differences between the different pectin samples. The obtained spectra in the wavelength region where pectin characteristic bands are typically detected (1700-600 cm^{-1}) are shown in Fig. 1. The bands located at 1022 and 1106 cm^{-1}, which are attributed to glycosidic linkages (C–C, C–O stretching bond, respectively) were observed in all the samples. Their appearance indicated that the pectin had high HG content (Baum et al., 2017; Méndez, Fabra, Gómez-Mascaraque et al., 2021). In addition, the band at 1046 cm^{-1}, indicative of the presence of neutral sugars, such as arabinose, xylose, and galactose (Baum et al., 2017) was also visible in OPA and OP extracts as a broad shoulder, although the relative intensity was not the same for all the enzymatically-treated samples, being significantly less intense for those in which the enzymatic hydrolysis included PME. This is related to the debranching and, thus, to the lower amount of neutral sugar side chains (as shown in Table 1) which were removed during the dialysis carried out after the enzymatic treatment. It should be noted that the relative intensity of this band also

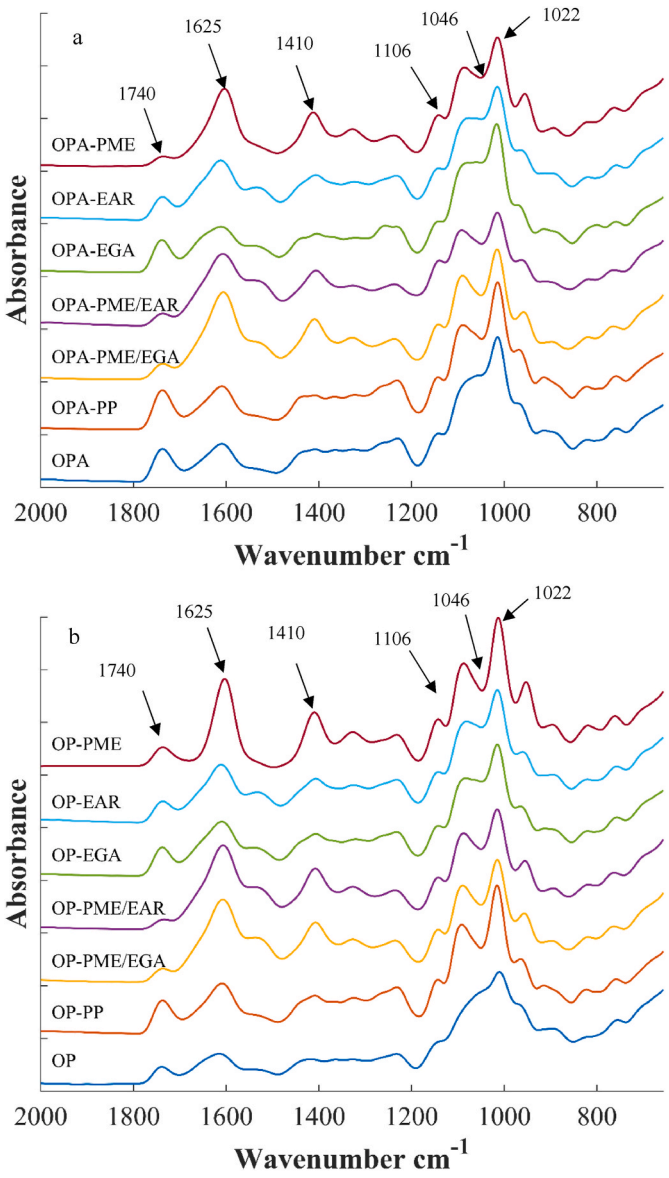

Fig. 1. FT-IR spectra from 600 to 2000 cm^{-1} (main relevant spectral range for pectin) of OPA (a) and OP (b) pectin after the different enzymatic treatments.

decreased after the PP treatment. All these results are in good agreement with the compositional analysis (cf. Table 1) and evidenced the presence of small amounts of AGP (Chen et al., 2016; Funami et al., 2011) which were lost after the proteolytic treatment.

In agreement with DE analysis (cf. Table 1), the relative intensity of the bands related to the free carboxyl groups COO^{-}, located at *ca.* 1625 cm^{-1}, and the weaker symmetric vibrating band centred at 1410 cm^{-1}(Baum et al., 2017; Karnik, Jung, Hawking, & Wicker, 2016), were clearly increased in the pectin samples hydrolysed with PME (alone or in combination with EAR or EGA), whereas the band centred at *ca.* 1740 cm^{-1}, ascribed to the vibration of the esterified carbonyl group C═O, decreased in PME-treated samples.

3.2. Rheological properties of pectin-based solutions and gels

3.2.1. Effect of de-branching on steady shear flow behavior

The rheological behavior of the native and enzymatically-treated pectin extracts was also evaluated and they were compared with a commercial low-methoxyl citrus pectin (LMCP) with a DE 5% in order to understand the role of pectin composition and structure on the viscosity

and gelling properties of the corresponding pectin. LMCP was chosen as a reference since it is well-known that low DE pectin have excellent gelling properties.

Complete flow curves presented in Fig. 2 show a shear-thinning behavior (pseudoplastic), which was accentuated in the more branched structures (OPA). The presence of highly branched pectin components contributed to the formation of chain entanglements, probably a higher hydrodynamic radius and, consequently, a higher pseudoplastic character of the pectin solution (Celus, Kyomugasho, Van Loey, Grauwet, & Hendrickx, 2018; Chan, Choo, Young, & Loh, 2017). The rheological data of the resulting solutions were accurately fitted to the Ostwald-de Waale model ($r^2 \sim 0.99$) and, the flow (n) and consistency (k) indexes together with the apparent viscosity (η_{ap}) values at a shear rate of 200 s^{-1} are summarized in Table 2. The flow index (n) indicates the degree of Non-Newtonian ($n < 1$) characteristics of the fluid whereas the consistency index gives an idea of the viscosity of the fluid. As a general observation, the enzymatic treatments promoted a decrease in the apparent viscosity and consistency index whereas the flow index increased. This result indicated that enzymatic digestion made the pectin solutions less viscous and less shear thinning, which again was related to the de-branching of OP and OPA. However, when

Table 2
Parameters of flow curves obtained by fitting the Ostwald–de Waele model for the different pectin at 2% (w/v).

Samples	n[b]	K	r^2	η_{ap} (Pa.s) at 200 s^{-1}
OPA	0.436	9.210	0.997	0.464
OPA-PME	0.314	20.566	0.991	0.543
OPA-EAR	0.899	0.022	0.990	0.013
OPA-EGA	0.764	0.150	0.998	0.043
OPA-PME/EAR	0.671	0.012	0.994	0.002
OPA-PME/EGA	0.306	4.510	0.980	0.114
OPA-PP	0.928	0.131	0.999	0.089
OP	0.780	0.057	0.995	0.018
OP-PME	0.889	0.103	0.999	0.057
OP-EAR	0.977	0.001	0.992	0.0009
OP-EGA	0.9205	0.013	0.9983	0.009
OP-PME/EAR	0.6709	0.0117	0.990	0.002
OP-PME/EGA	0.841	0.0196	0.990	0.009
OP-PP	0.866	0.006	0.999	0.003
LMCP[a]	0.9898	0.032	0.999	0.030

[a] Citrus pectin with 5% DE.
[b] Depending on the value of the flow index (n), the fluid can be classified as being pseudoplastic ($n < 1$), Newtonian ($n = 1$), or dilatant ($n > 1$).

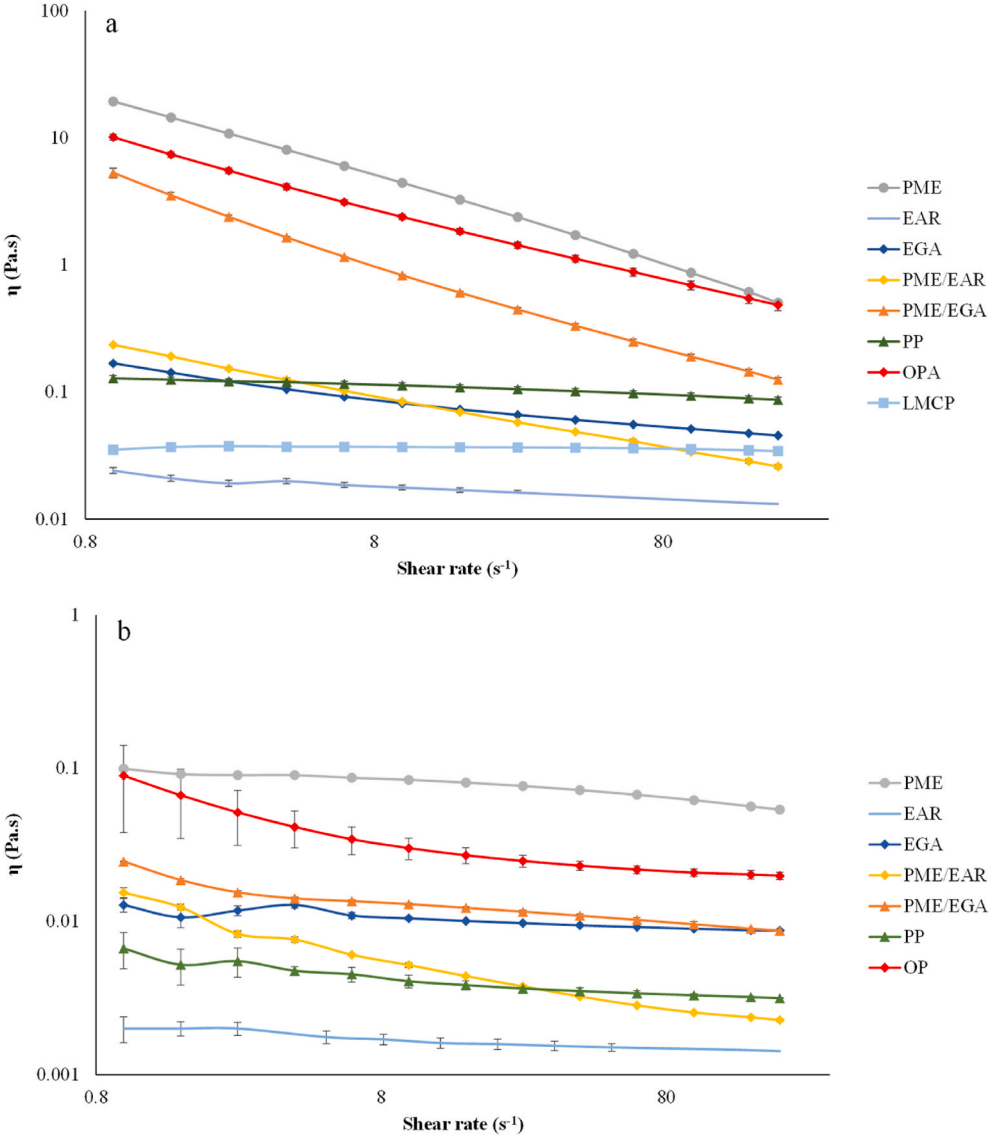

Fig. 2. Apparent viscosity of enzymatically treated, a) OPA, and b) OP watermelon rind pectin samples at a concentration of 2% (w/v). Commercial LMCP is also shown for comparison.

(OPA or OP) were enzymatically treated only with PME, they were more viscous and more shear thinning that their untreated counterparts. This is probably ascribed to the presence of a higher amount of non-esterified groups which are able to form strong interactions (most likely hydrogen bonds) with the neutral sugar side chains. Uncharged carboxyl groups may form hydrogen bonds inside the polymer molecule and between two neighboring chains (Gawkowska, Cybulska, & Zdunek, 2018; Walkinshaw & Arnott, 1981). Additionally, the removal of the lower molecular weight fraction of these neutral sugar side chains might further increase the viscosity and shear-thinning behavior. This is in line with the DE values and compositional analysis. These results further confirmed that the molecular structure of pectin significantly affect the steady-shear flow behavior of the resulting solutions, i.e. longer sugar side chains provided more viscous solutions by means of chain entanglements (Chan et al., 2017; Méndez, Fabra, Martínez-Abad et al., 2021).

As observed in Fig. 2, the viscosity of the pectin modified with EAR was significantly lower from other enzymatic modifications. This is explained by the loss of arabinan structures or external arabinosyl residues (see Table 1), which confer pectin with a higher hydrophilic character and higher water holding capacity (Ramasamy, Gruppen, & Kabel, 2015).

Finally, a LMCP solution was also prepared as a reference and compared with WRP solutions. As seen in Table 2, it behaved near to a Newtonian fluid, supporting the key role of sugar side chains on the rheological behavior.

3.2.2. *Dynamic-viscoelastic behavior of enzymatically-treated pectin*

The effect of the enzymatic treatment in the gel properties of the different pectin fractions with Ca^{2+} divalent ions was investigated by performing dynamic oscillatory tests. G' and G'' were measured as a function of frequency (rad·s^{-1}), at a fixed strain depending on previous amplitude sweep tests. As a general observation, the presence of long branched side chains decreased the gelation capacity of pectin, indicating that the presence of less branched non-methyl esterified galacturonic acid chains facilitated their association with the divalent ions to originate the network structures responsible for hydrogel formation. In fact, very weak hydrogels were formed with the pure pectin extracts (OPA and OP). However, this gelling network was lost in ERA and EGA treated samples in which the results revealed that the G' was higher than G'' only at low angular frequency range (<1 rad/s). This corresponds to the loss of solid-related and elastic gel-like properties in these samples, as it was further confirmed by SAXS, and suggests that both the presence of longer sugar side chains in RG, as evidenced by the higher RB ratio (which refers to the side chain length) together with the high content of methyl esterified galacturonic acid chains negatively affected the interactions between the negative charge of non-esterified groups and Ca^{2+}.

As observed from Fig. 3, all hydrogels formed with PME-treated samples exhibited a storage modulus (G') higher than the loss modulus (G''), denoting that the elastic character was always dominant when a load was applied and evidencing the formation of a packaged gelling network by means of the electrostatic interactions through cooperative binding of the Ca^{2+} to the non-methyl esterified galacturonic acid (NMGalA) blocks, as later supported by SAXS (see section 3.3) and in agreement with the gel strength values of the hydrogels formed (see Supplementary Material S1). There were not great differences between G' values of the hydrogels formed with only PME-treated OP or OPA samples, suggesting that, even though more linear backbone with low DE values facilitated the generation of Ca^{2+} gel networks, the presence of some sugar side chains (higher RB values for OPA-PME samples) could play an important role as reinforcement in hydrogels formed by means of intermolecular associations. Similar behavior was also found in a previous work, where regardless of Ca^{2+} concentration, a reduction in polymer chain entanglements in de-branched pectin, provoked a drastic reduction of the gel strength in carrot pectin

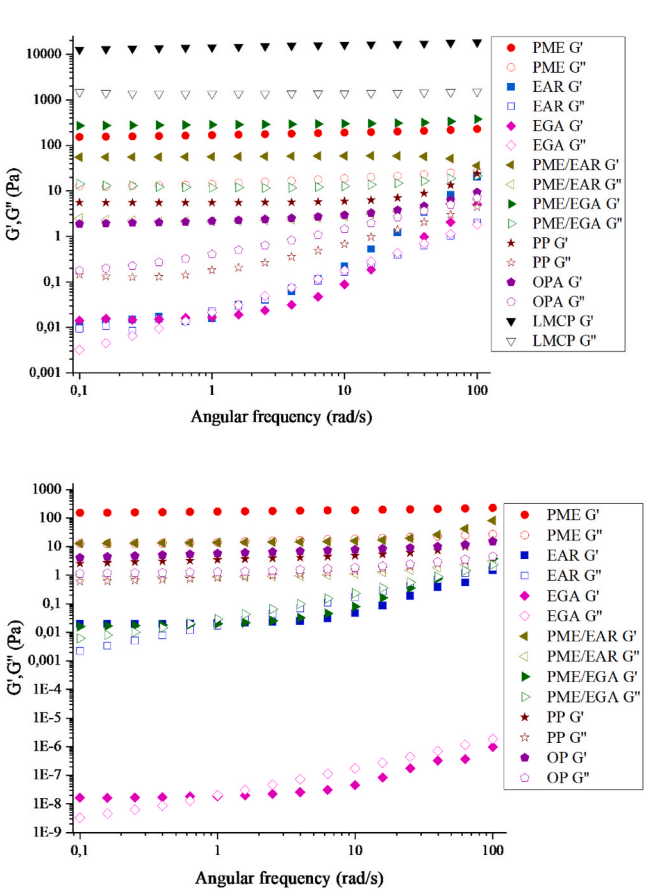

Fig. 3. Dynamical oscillatory frequency sweep test curves of Ca^{2+} gels enzymatically modified from OPA (a) and OP (b) pectin. plot of storage modulus (G'), loss modulus (G'') vs. angular frequency. Filled and open symbols correspond to G' and G'' respectively. LMCP corresponds to low methoxy citrus pectin used for comparison.

(Ngouémazong et al., 2012).

With regards to the samples treated with both enzymes, stronger hydrogels were formed for OPA, being higher in those treated with PME/EGA. This is consistent with the hypothesis of small sugar side chains, being able to promote the intermolecular association of polymer chains through hydrogen bonding.

Based on these experimental results, it seems that in the presence of Ca^{2+}, a rapid cooperative binding of Ca^{2+} to the NMGalA blocks is stimulated throughout the polymer, thereby generating a number of energetically stable and strong junction zones. However, it is postulated that in the de-branched and de-methyl-esterified pectin, although a similar size and distribution of NMGalA blocks through the polymer could occur in PME/EGA and PME/EGA treated samples, there is a certain critical DE value in which the presence of short branched chains favour the formation of side chain entanglements, thereby increasing the overall entanglement of the polymer and thus, resulting in stronger gels. This effect is schematically represented in Fig. 4.

When pectin extracts were treated with proteolytic enzymes, stronger hydrogels were observed in OP-PP treated samples which can be ascribed to the removal of smaller protein-arabinogalactan complexes in equal amounts, thus favoring the accessibility of Ca^{2+} ions to the non-esterified acid groups (see Table 1). In contrast, OPA-PP gels behaved similar to its OPA counterpart.

3.3. *Nanostructural characterization of pectin gels*

To investigate the effect of the different enzymatic treatments on the

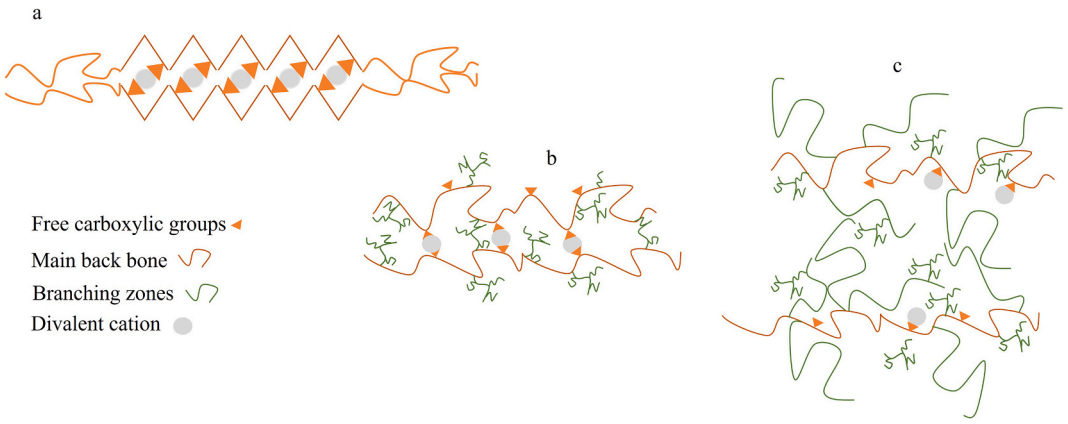

Fig. 4. Schematic representation for pectin hydrogels proposed for (a) LMCP, (b) low DE and RB pectin (i.e. PA-PME/EGA) and (c) high DE and RB pectin (i.e. OPA/EGA).

nanostructure of the pectin, gelling formulations were characterized by means of SAXS and the obtained patterns are shown in Fig. 5. When comparing the patterns from the untreated pectin (OP and OPA) with the commercial citrus pectin, it was evident that while the citrus pectin showed a marked broad shoulder feature, indicative of the formation of a gelling network, the untreated pectin showed very weak scattering features, which can be more clearly visualized in the corresponding Kratky plots (cf. Fig. S2). The patterns from OP and OPA pectin are similar to those previously reported for pectin solutions at concentrations at which intermolecular interactions take place (Méndez, Fabra, Martínez-Abad et al., 2021). In particular, one broad shoulder-like feature appears within the low-q region ($q < \sim 0.03$ Å^{-1}), which is associated to intermolecular interactions and chain clusters, and a more marked shoulder is observed within the high-q region, which originates from the scattering of rod-like pectin chains. Interestingly, the unmodified OPA and OP pectin showed almost identical patterns, indicating their similarity at the nanoscale level. The scattering data were fitted using different empirical models and the obtained fitting parameters are gathered in Table 3. As observed, the OPA and OP pectin showed very similar structural parameters, with power-law exponents around 3 within the whole q range studied, denoting the existence of mass fractals, in particular, clustered networks. This means that, at the size range covered by the SAXS experiments, none of the samples showed a linear rod-like structure, but instead they presented branched networks. In fact, the Rg_3 values, characteristic of the cross-section of rod-like pectin chains, were around 6 nm, much larger than the typical cross-sections reported for pectin rod-like structures (Méndez, Fabra, Martínez-Abad et al., 2021). On the other hand, the Rg_2 values, characteristic of the size of the molecular clusters, were around 18–23 nm, which is in agreement with previous studies (Alba, Bingham, Gunning, Wilde, & Kontogiorgos, 2018; Méndez, Fabra, Martínez-Abad et al., 2021).

As evidenced by the results shown in Fig. 5B and C, the enzymatic treatments seemed to have a stronger effect on the nanostructure of the OP pectin samples. In particular, the OP-EAR and OP-EGA samples showed a significant decrease in the scattering intensity, suggesting that the physical density of the samples may have been decreased as a result of weaker intermolecular networks being formed. On the contrary, the PME treatment led to a slight increase in the scattering intensity and the low-q shoulder was not observed. The fact that this scattering feature was not detected may be a consequence of a larger interfacial scattering length density contrast (i.e. greater contrast between the pectin network and the surrounding solvent) or simply because the scattering feature appeared at lower q values out of the covered range. In any case, this may be indicative of the formation of a more densely packed gelling network, more similar to that observed for the citrus pectin. The enzymatic treatments with PME/EGA, PME/EAR and PP did not produce strong modification on the nanostructure, although there was a slight reduction in the mesh size of the gel network and in the radius of gyration associated to the rod-like pectin chains.

In the case of the OPA pectin samples, although the enzymatic treatments did not produce strong changes in the scattering intensity of the samples, some of the applied treatments induced the formation of different types of nanostructures to those observed in the unmodified OPA sample. In particular, the EGA treatment had the strongest effect, hindering the formation of intermolecular networks, similarly to what was observed for the OP-EAR and OP-EGA samples. On the other hand, all the PME treated samples showed a distinct behaviour, with slightly higher scattering intensity than the unmodified OPA pectin and the low-q scattering feature being absent. This might be indicative of the formation of stronger gelling networks in these samples, in agreement with the rheological characterization.

4. Conclusions

In this work, two watermelon rind pectin extracts (OP and OPA) were enzymatically modified using six different treatments, including de-esterification, de-branching of arabinose and galactose side chains, their combinations and de-proteinization. The compositional analyses indicated that the de-esterification and its combination with be-branching enzymes had the most significant impact on the pectin structure, greatly reducing the esterification degree (DE) of both pectin extracts and significantly modifying the linearity and branching ratios. Furthermore, the proteolytic enzymes hydrolysed the protein moieties linked to the arabinogalactan part of pectin, which results in a significant increase in the linearity in both OP-PP and OPA-PP samples. This effect was more accentuated in OP-PP samples in which the arabinogalactan-protein (AGP) fragments were removed in equal amounts.

The presence of highly branched pectin components contributed to the formation of chain entanglements and, consequently, to a higher pseudoplastic character of the pectin solution. In general, enzymatic treatments made the pectin solutions less viscous and less shear thinning. Pectin solutions in which carbohydrates were enzymatically treated only with PME, were more viscous and more shear thinning than their untreated counterparts. The presence of long branched side chains and high methyl esterified galacturonic acid chains promoted the formation of weaker hydrogels whereas de-esterification of the original pectin enabled intermolecular association giving rise to more viscous solutions and stronger hydrogels with the formation of ordered and densely packed structures. However, after de-esterifying and de-branching the galacturonic side chains, the presence of small arabinogalactans side chains in the pectin extracts could act as reinforcement agents, inducing the formation of more densely packed networks and stronger hydrogels.

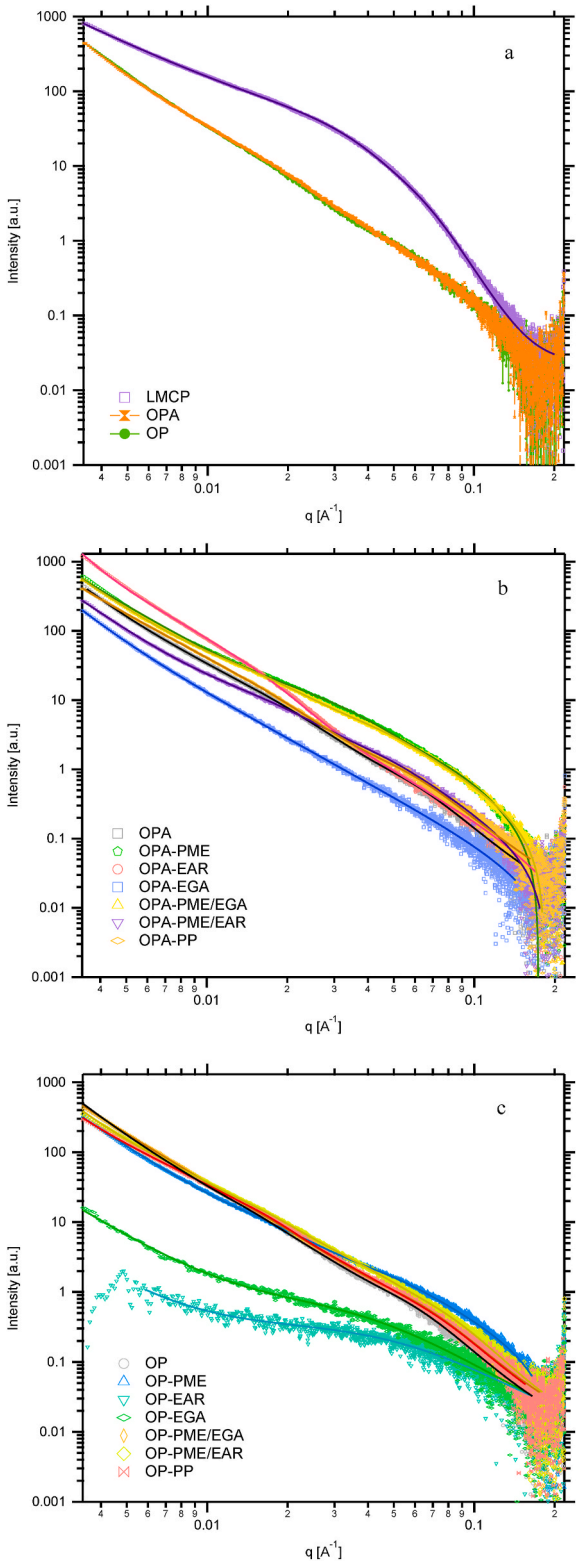

Fig. 5. SAXS patterns from the pectin samples. (a) OPA and OP pectin compared to the low methoxy citrus pectin. (b) OPA enzymatically modified pectin. (c) OP enzymatically modified pectin. Markers represent the experimental data and solid lines show the fits obtained using the corresponding fitting models.

Table 3
Parameters obtained from the fits of the SAXS data for the different pectin samples.

	Unified model					Correlation length		
Samples	P_1	Rg_2 (nm)	P_2	Rg_3 (nm)	P_3	n	m	ξ_L (nm)
OPA	2.9	18.3	3.2	6.2	3.3	–	–	–
OPA-PME	–	–	2.4	5.1	2.5	–	–	–
OPA-EAR	3.6	24.0	3.5	3.2	3.8	–	–	–
OPA-EGA	–	–	–	–	–	2.7	2.0	6.2
OPA-PME/EGA	–	–	2.6	9.5	2.1	–	–	–
OPA-PME/EAR	–	–	2.7	8.9	2.3	–	–	–
OPA-PP	2.6	22.0	3.1	6.6	3.1	–	–	–
OP	3.0	23.4	3.4	6.3	3.4	–	–	–
OP-PME	–	–	2.6	8.6	1.9	–	–	–
OP-EAR	–	–	–	–	–	2.4	2.2	1.8
OP-EGA	–	–	–	–	–	2.3	2.4	2.4
OP-PME/EGA	2.6	20.6	3.5	5.9	3.3	–	–	–
OP-PME/EAR	3.0	19.4	3.7	4.5	3.7	–	–	–
OP-PP	2.9	19.6	4.0	5.4	3.4	–	–	–
LMCP	–	–	2.4	9.3	4.0	–	–	–

Unified model: P_i: power-law coefficient for the structural level i; Rg_2: radius of gyration associated to the structural level i (i = 1,2,3).
Correlation length model: n: power-law exponent; m: Lorentzian exponent; ξ_L: correlation length.

Thus, enzymes acting on neutral sugar side chains (EAR and EGA) alone were not capable of debranching the pectin structure, resulting in weaker gels. In contrast, PME-treated samples might break electrostatic interaction between smaller sugar side chains and these were removed during dialysis, especially in OP, which resulted more viscous solutions and stronger gels. When both enzymes were combined, debranching produced the strongest gels similar to the benchmark LMCP. However, composition and SAXS analysis revealed that the gelling mechanisms involved densely packed structures where the small side chains remaining in the OPA acted as reinforcement. PP treatment had a greater impact on OP samples by removing small AGP fractions.

Understanding the gelation mechanism of WRP hydrogels depending on its composition and structure and their implication on the nanostructure will open the possibility of designing hydrogels with specific properties for targeted applications, such as encapsulation systems for the controlled release of bioactive compounds. Therefore, the composition and structure of WRP can be tailored depending on the final intended used such as thickeners, gelling or stabilizing additives in food. These results evidence that enzymatic treatments greatly modified the composition and structure of watermelon pectin extracts and provide the basis for a rational design of pectin hydrogels depending of the targeted applications within the food industry.

Declaration of competing interest

The authors declare that they have no known competing financial interests or personal relationships that could have appeared to influence the work reported in this paper.

Data availability

Data will be made available on request.

Acknowledgments

Grant RTI-2018-094268-B-C22 funded by MCIN/AEI/10.13039/501100011033 and by "ERDF A way of making Europe". This work was also funded by the grant INNVAL10-19-009 - CA8250 from Agència Valenciana d'Innovació (AVI). D.A. Méndez. is supported by the

Administrative Department of Science, Technology and Innovation (Colciencias) of the Colombian Government (783–2017). This research is part of the CSIC program for the Spanish Recovery, Transformation and Resilience Plan funded by the Recovery and Resilience Facility of the European Union, established by the Regulation (EU) 2020/2094. Interdisciplinary Platform for Sustainable Plastics towards a Circular Economy+. (PTI-SusPlast+) is also acknowledged for financial support.

Appendix A. Supplementary data

Supplementary data to this article can be found online at https://doi.org/10.1016/j.foodhyd.2022.108119.

References

Alba, K., Bingham, R. J., Gunning, P. A., Wilde, P. J., & Kontogiorgos, V. (2018). Pectin conformation in solution. *Journal of Physical Chemistry B, 122*(29), 7286–7294. https://doi.org/10.1021/acs.jpcb.8b04790. research-article.

Baum, A., Dominiak, M., Vidal-Melgosa, S., Willats, W. G. T. T., Søndergaard, K. M., Hansen, P. W., et al. (2017). Prediction of pectin yield and quality by FTIR and carbohydrate microarray analysis. *Food and Bioprocess Technology, 10*(1), 143–154. https://doi.org/10.1007/s11947-016-1802-2

Beaucage, G. (1995). Approximations leading to a unified exponential/power-law approach to small-angle scattering. *Journal of Applied Crystallography, 28*(6), 717–728. https://doi.org/10.1107/s0021889895005292

Beaucage, G. (1996). Small-angle scattering from polymeric mass fractals of arbitrary mass-fractal dimension. *Journal of Applied Crystallography, 29*(2), 134–146. https://doi.org/10.1107/S0021889895011605

Bindereif, B., Eichhöfer, H., Bunzel, M., Karbstein, H. P., Wefers, D., & van der Schaaf, U. S. (2021). Arabinan side-chains strongly affect the emulsifying properties of acid-extracted sugar beet pectins. *Food Hydrocolloids, 121*. https://doi.org/10.1016/J.FOODHYD.2021.106968

Campbell, M. (2006). *Extraction of pectin from watermelon rind.* Oklahoma State University.

Capel, F., Nicolai, T., Durand, D., Boulenguer, P., & Langendorff, V. (2006). Calcium and acid induced gelation of (amidated) low methoxyl pectin. *Food Hydrocolloids, 20*(6), 901–907. https://doi.org/10.1016/j.foodhyd.2005.09.004

Celus, M., Kyomugasho, C., Van Loey, A. M., Grauwet, T., & Hendrickx, M. E. (2018, November 1). Influence of pectin structural properties on interactions with divalent cations and its associated functionalities. *Comprehensive Reviews in Food Science and Food Safety*. https://doi.org/10.1111/1541-4337.12394. Blackwell Publishing Inc.

Chan, S. Y., Choo, W. S., Young, D. J., & Loh, X. J. (2017, April 1). Pectin as a rheology modifier: Origin, structure, commercial production and rheology. *Carbohydrate Polymers*. https://doi.org/10.1016/j.carbpol.2016.12.033. Elsevier Ltd.

Chen, H., Qiu, S., Gan, J., Liu, Y., Zhu, Q., & Yin, L. (2016). New insights into the functionality of protein to the emulsifying properties of sugar beet pectin. *Food Hydrocolloids, 57*, 262–270. https://doi.org/10.1016/j.foodhyd.2016.02.005

Denman, L. J., & Morris, G. A. (2015). An experimental design approach to the chemical characterisation of pectin polysaccharides extracted from Cucumis melo Inodorus. *Carbohydrate Polymers, 117*, 364–369. https://doi.org/10.1016/j.carbpol.2014.09.081

Doungla, E., & Vandebril, S., … , … (2009). Quick and reliable method of preparation of strong homogeneous calcium-pectin gels. *Symposium of Foods*, 2–3. Retrieved from https://lirias.kuleuven.be/handle/123456789/301835.

FAOSTAT. (2021). *CROPS*. Retrieved. from http://www.fao.org/faostat/en/#data/QC/visualize. (Accessed 27 May 2021).

Funami, T., Nakauma, M., Ishihara, S., Tanaka, R., Inoue, T., & Phillips, G. O. (2011). Structural modifications of sugar beet pectin and the relationship of structure to functionality. *Food Hydrocolloids, 25*(2), 221–229. https://doi.org/10.1016/j.foodhyd.2009.11.017

Funami, T., Zhang, G., Hiroe, M., Noda, S., Nakauma, M., Asai, I., et al. (2007). Effects of the proteinaceous moiety on the emulsifying properties of sugar beet pectin. *Food Hydrocolloids, 21*(8), 1319–1329. https://doi.org/10.1016/j.foodhyd.2006.10.009

Gawkowska, D., Cybulska, J., & Zdunek, A. (2018). Structure-related gelling of pectins and linking with other natural compounds: A review. *Polymers, 10*(7), 762. https://doi.org/10.3390/polym10070762

Hartati, I., & Subekti, E. (2015). Microwave assisted extraction of watermelon rind pectin. *International Journal of ChemTech Research, 8*(11), 163–170.

Houben, K., Jolie, R. P., Fraeye, I., Van Loey, A. M., & Hendrickx, M. E. (2011). Comparative study of the cell wall composition of broccoli, carrot, and tomato: Structural characterization of the extractable pectins and hemicelluloses. *Carbohydrate Research, 346*(9), 1105–1111. https://doi.org/10.1016/j.carres.2011.04.014

Hromadová, D., Soukup, A., & Tylová, E. (2021). Arabinogalactan proteins in plant roots - an update on possible functions. *Frontiers of Plant Science, 12*. https://doi.org/10.3389/FPLS.2021.674010

Ilavsky, J., & Jemian, P. R. (2009). Irena: Tool suite for modeling and analysis of small-angle scattering. *Journal of Applied Crystallography, 42*(2), 347–353. https://doi.org/10.1107/S0021889809002222

Karnik, D., Jung, J., Hawking, S., & Wicker, L. (2016). Sugar beet pectin fractionated using isopropanol differs in galacturonic acid, protein, ferulic acid and surface hydrophobicity. *Food Hydrocolloids, 60*, 179–185. https://doi.org/10.1016/j.foodhyd.2016.03.037

Kieffer, J., & Ashiotis, G. (2014). PyFAI: A Python library for high performance azimuthal integration on GPU. *Powder Diffraction, 28*(SUPPL.2), 3. Retrieved from http://arxiv.org/abs/1412.6367.

Klavons, J. A., & Bennett, R. D. (1986). Determination of methanol using alcohol oxidase and its application to methyl ester content of pectins. *Journal of Agricultural and Food Chemistry, 34*(4), 597–599. https://doi.org/10.1021/jf00070a004

Lara-Espinoza, C., Carvajal-Millán, E., Balandrán-Quintana, R., López-Franco, Y., & Rascón-Chu, A. (2018). April 18). Pectin and pectin-based composite materials: Beyond food texture. *Molecules. MDPI AG*. https://doi.org/10.3390/molecules23040942

Lee, K. Y., & Choo, W. S. (2020). Extraction optimization and physicochemical properties of pectin from watermelon (Citrullus lanatus) rind: Comparison of hydrochloric and citric acid extraction. *Journal of Nutraceuticals and Food Science, 5*(1), 1. https://doi.org/10.36648/nutraceuticals.5.1.1

Méndez, D. A., Fabra, M. J., Gómez-Mascaraque, L., López-Rubio, A., & Martinez-Abad, A. (2021). Modelling the extraction of pectin towards the valorisation of watermelon rind waste. *Foods, 10*(4), 738. https://doi.org/10.3390/foods10040738

Méndez, D. A., Fabra, M. J., Martínez-Abad, A., Martínez-Sanz, Gorria, M., & López-Rubio, A. (2021). Understanding the different emulsification mechanisms of pectin: Comparison between watermelon rind and two commercial pectin sources. *Food Hydrocolloids, 120*, Article 106957. https://doi.org/10.1016/j.foodhyd.2021.106957

Nakauma, M., Funami, T., Noda, S., Ishihara, S., Al-Assaf, S., Nishinari, K., et al. (2008). Comparison of sugar beet pectin, soybean soluble polysaccharide, and gum Arabic as food emulsifiers. 1. Effect of concentration, pH, and salts on the emulsifying properties. *Food Hydrocolloids, 22*(7), 1254–1267. https://doi.org/10.1016/j.foodhyd.2007.09.004

Ngouémazong, D. E., Kabuye, G., Fraeye, I., Cardinaels, R., Van Loey, A., Moldenaers, P., et al. (2012). Effect of debranching on the rheological properties of Ca2+-pectin gels. *Food Hydrocolloids, 26*(1), 44–53. https://doi.org/10.1016/j.foodhyd.2011.04.009

Ognyanov, M., Georgiev, Y., Petkova, N., Ivanov, I., Vasileva, I., & Kratchanova, M. (2018). Isolation and characterization of pectic polysaccharide fraction from in vitro suspension culture of Fumaria officinalis L. *International Journal of Polymer Science, 2018*, 1–13. https://doi.org/10.1155/2018/5705036

Oosterveld, A., Voragen, A. G. J., & Schols, H. A. (2002). Characterization of hop pectins shows the presence of an arabinogalactan-protein. *Carbohydrate Polymers, 49*(4), 407–413. https://doi.org/10.1016/S0144-8617(01)00350-2

Petkowicz, C. L. O., Vriesmann, L. C., & Williams, P. A. (2017). Pectins from food waste: Extraction, characterization and properties of watermelon rind pectin. *Food Hydrocolloids, 65*, 57–67. https://doi.org/10.1016/j.foodhyd.2016.10.040

Prakash Maran, J., Sivakumar, V., Thirugnanasambandham, K., & Sridhar, R. (2014). Microwave assisted extraction of pectin from waste Citrullus lanatus fruit rinds. *Carbohydrate Polymers, 101*(1), 786–791. https://doi.org/10.1016/j.carbpol.2013.09.062

Ramasamy, U. R., Gruppen, H., & Kabel, M. A. (2015). Water-holding capacity of soluble and insoluble polysaccharides in pressed potato fibre. *Industrial Crops and Products, 64*, 242–250. https://doi.org/10.1016/J.INDCROP.2014.09.036

Schols, H. A., & Voragen, A. G. J. (2003a). Pectic polysaccharides. In J. R. Whitaker, A. G. J. Voragen, & D. W. S. Wong (Eds.), *Handbook of food enzymology* (Vol. 353, pp. 829–843). New York, NY: Dekker. https://doi.org/10.1201/9780203910450-68.

Schols, H. A., & Voragen, A. G. J. (2003b). Pectins and their manipulation. In G. B. Seymour, & J. P. Knox (Eds.), *Pectins and their manilpulation* (p. 29). Oxford: Blackwell. Retrieved from https://library.wur.nl/WebQuery/wurpubs/326288.

Verhoef, R., Lu, Y., Knox, J. P., Voragen, A. G. J., & Schols, H. A. (2009). Fingerprinting complex pectins by chromatographic separation combined with ELISA detection. *Carbohydrate Research, 344*(14), 1808–1817. https://doi.org/10.1016/j.carres.2008.09.030

Voragen, A. G. J. J., Coenen, G.-J. J., Verhoef, R. P., & Schols, H. A. (2009). Pectin, a versatile polysaccharide present in plant cell walls. *Structural Chemistry, 20*(2), 263–275. https://doi.org/10.1007/s11224-009-9442-z

Walkinshaw, M. D., & Arnott, S. (1981). Conformations and interactions of pectins: I. X-Ray diffraction analyses of sodium pectate in neutral and acidified forms. *Journal of Molecular Biology, 153*(4), 1055–1073. https://doi.org/10.1016/0022-2836(81)90467-8

Wiles, P. G., Gray, I. K., Kissling, R. C., Delahanty, C., Evers, J., Greenwood, K., et al. (1998). Routine analysis of proteins by Kjeldahl and Dumas methods: Review and Interlaboratory study using dairy products. *Journal of AOAC International, 81*(3), 620–632. https://doi.org/10.1093/jaoac/81.3.620